

Loss of stability of low-mass stars through neutronization

M. M. Basko and V. S. Imshennik

Institute of Applied Mathematics, USSR Academy of Sciences, Moscow

(Submitted July 4, 1974)

Astron. Zh. 52, 469–480 (March–April 1975)

The results are reported of numerical calculations for the terminal evolutionary phase and the loss of mechanical stability in iron cores with masses of 1.21, 1.4, and 1.7 M_{\odot} . Exact equations are applied to establish the thermodynamics of the radiation and the electron-positron gas. The chemical composition at $T \gtrsim 3 \cdot 10^9$ K is determined from the condition of statistical equilibrium over the nuclei. The kinetics of β processes is systematically taken into account. A polytropic density distribution with $n = 3$ is adopted to obtain an approximate solution of the hydrodynamical equations. In the 1.7 and 1.4 M_{\odot} models there is a well-defined epoch at which mechanical stability is lost and the transition to the hydrodynamic-collapse phase occurs. In the 1.21 M_{\odot} model, however, no such epoch exists; the evolution of the core on the characteristic time scale of the β processes gradually accelerates to the collapse phase. In all the models, but particularly for 1.21 M_{\odot} , the thermodynamic-nonequilibrium nature of the β processes is highly significant as it causes the entropy to rise in the central zone. The predominant contribution to the energy-loss rate in all the models is supplied by URCA neutrino radiation. The possible formation of submassive ($M < 1.0 M_{\odot}$) neutron stars is discussed.

PACS numbers: 97.10.D, 97.70.Q

1. INTRODUCTION

When a sufficiently massive star (having a core of mass $M \gtrsim 5 M_{\odot}$) exhausts its supply of the nuclear fuel,¹ its central temperature T_c will reach $\approx 10^{10}$ K and it will become mechanically unstable because of photodissociation of the nuclei of the iron-peak elements, which serves to reduce the adiabatic index of the material to values $\gamma < 4/3$. Stability will also be lost below a mass of $5 M_{\odot}$ down to the Chandrasekhar mass limit (1.1–1.4 M_{\odot}), depending on the chemical composition of the core, but neutronization of the material will now be responsible for the loss of stability. The relative contribution of the photodissociation and neutronization processes depends significantly on the structure of the stellar core, for a specified mass.

Several authors^{2–6} have recently performed calculations of the late evolutionary stages of main-sequence stars with masses in the range $64 M_{\odot} \gtrsim M_{\text{ms}} \gtrsim 4 M_{\odot}$. It has been found that these stars will terminate their evolution with a central iron core of mass $3 M_{\odot} \gtrsim M_{\text{Fe}} \gtrsim 1 M_{\odot}$. The question of the limiting mass of the iron core has received intensive discussion,^{7,8} especially with regard to the lower limit of M_{Fe} . Neuchi et al.^{3,4} conclude that at the center of carbon–oxygen stars with masses $M_{\text{CO}} = 5 M_{\odot}$ and $2.6 M_{\odot}$, iron cores with masses $M_{\text{Fe}} = 1.7 M_{\odot}$ and $1.4 M_{\odot}$, respectively, will be formed. Note that such a carbon–oxygen core can be much less massive than the main-sequence star, quite apart from mass loss during the evolutionary process; for example, $M_{\text{CO}} = 2.6 M_{\odot}$ corresponds to $M_{\text{ms}} = 16 M_{\odot}$ on the main sequence.^{4,5}

The central density ρ_c at which instability sets in increases rapidly toward stars of lower mass. Stars with $M_{\text{CO}} \leq 2.6 M_{\odot}$ will lose their stability at $\rho_c \gtrsim 10^9$ g/cm³. At densities as high as these the role of photodissociation will diminish, and processes whereby the matter becomes neutronized (that is, β processes) will begin to exert a major influence on the stability of the star. As they take place rather slowly (compared to photonuclear reactions and

hydrodynamical processes) and not in thermodynamic equilibrium (for neutrinos and antineutrinos can freely escape from the star), these β processes can significantly alter the mode of stability loss in the stellar core.

In this connection the concept of an adiabatic index γ_1 for a "frozen" ratio of the total neutron and proton population was introduced and substantial in the previous paper.⁹ Calculations have shown that in the high-density range $\rho_c \gtrsim 10^9$ g/cm³ the index $\gamma_1 \gtrsim 4/3$, although it differs very little from the critical value $4/3$. Accordingly, under such conditions instability can develop with the characteristic time scales of the β processes which, as we have mentioned, considerably exceed the hydrodynamic time.^{1,10}

We shall investigate below the role of β processes in the development of instability for iron stars of low mass, with $1.2 M_{\odot} \leq M_{\text{Fe}} \leq 1.7 M_{\odot}$. Unlike the case in a previous analysis,¹¹ β processes will here be taken much more accurately into account, and the transition away from evolution to hydrodynamic contraction will itself be considered. The lower bound on the mass of the stars in question should naturally exceed the Chandrasekhar limit for a cool iron star. This limit¹² is 1.11 M_{\odot} . Our upper bound has been taken to be low enough so that β processes will still play a significant role in the subsequent evolution.

During the terminal evolutionary phase of the star, β processes (e^{\pm} captures and decays) will be accompanied by the following effects. 1) In addition to all the other energy-loss mechanisms (including neutrino losses), URCA neutrino losses will occur. 2) Electron capture will serve to diminish the pressure in the central regions of the star, shifting its equilibrium state toward higher densities and temperatures. 3) The nonequilibrium character of the β processes will cause the entropy to rise and the electron gas to be heated.^{10,13} It is important to recognize here that not just the thermodynamic equilibrium but also the kinetic equilibrium of the β processes will be violated, which in general is not possible because the free escape of neutrinos from the star. 4) The β processes will serve

to alter the chemical composition in the central regions of the star (nuclei overloaded with neutrons will appear), and this change will have a reciprocal effect on the β processes and the processes of nuclear photodissociation.

Our purpose in this paper is to clarify what influence all these effects will have on the course of the terminal evolution and on the loss of mechanical stability for low-mass stars. Finally, it is worth inquiring whether the evolution of a star with a sufficiently low mass ($M_{Fe} \leq 2 M_{\odot}$) can proceed in a quiescent, hydrostatic-equilibrium mode to the formation of a neutron star in the characteristic time for β processes at high densities.

2. DENSITY PROFILES AND STRUCTURAL EQUATIONS

As we have mentioned, an iron core (properly speaking, a core composed of iron-peak elements) with a mass $M \approx 1-2 M_{\odot}$ will be formed in the terminal evolutionary phase of an intermediate-mass main-sequence star ($M_{MS} \approx 4-16 M_{\odot}$). If the mass of the resulting core exceeds the Chandrasekhar mass M_{Ch} , then from some time onward the further evolution of the core will entail a loss of mechanical stability and collapse, independently of the state of the outer envelope. We may therefore confine attention to the dynamics of the iron core alone, and by the "star" we shall henceforth mean just the core.

In the mass range $1.2 M_{\odot} \leq M \leq 1.7 M_{\odot}$ that we are considering, iron stars will have a central density so high that the electron gas is ultrarelativistic and degenerate. Hence the structure of the star may be satisfactorily described by a polytrope with index $n = 3$. Calculations of the late evolutionary phases of carbon-oxygen stars²⁻⁴ confirm this representation.

Our principal simplifying assumption will be as follows. The hydrostatic-equilibrium evolution and the transition to the hydrodynamic collapse phase proceed along sequences of configurations with a density distribution corresponding to a polytrope $n = 3$:

$$\rho(t, q) = \rho_c(t) \psi^3(q). \quad (1)$$

Here the mass fraction q of the star plays the role of a Lagrangian coordinate, and the Lane-Emden function $\psi(q)$ satisfies the system of equations¹

$$\begin{cases} \psi'(q) = -\mu_1^2 q \psi^{-3}(q) \psi^{-4}(q) \\ \psi''(q) = \mu_1 \psi^{-3}(q) \psi^{-2}(q) \end{cases} \quad (2)$$

for boundary conditions $\psi(0) = 1$, $\psi'(0) = 0$. The constant $\mu_1 = 2.01824$ is determined from the condition $\psi(1) = 0$. The function $\psi(q)$ is related to the radius $r(t, q)$ for the Lagrangian coordinate q by

$$r(t, q) = R(t) [\psi(q)/\psi(1)], \quad (3)$$

where $R(t)$ is the radius of the star and $\psi(1) = 6.897$. Since the effective adiabatic index γ will necessarily remain close to its critical value $4/3$ throughout the development of instability in the star, it is justifiable to adopt a polytropic density profile with index $n = 3$. A polytrope with this index is noteworthy in that its hydrostatic equilibrium will not be violated if it contracts or expands homologously. The entire contraction of the star up to the hydrody-

amic collapse phase itself may therefore be satisfactorily approximated with such a profile. A similar approach has been adopted by Bisnovatyi-Kogan¹⁴ to study explosions of supermassive stars.

The complete system of equations describing the mass motion and structure of the star has the form

$$\frac{\partial^2 r}{\partial t^2} = -4\pi v^2 \frac{\partial p}{\partial m} - \frac{Gm}{r^2}, \quad (4)$$

$$\frac{\partial r}{\partial m} = \frac{1}{4\pi \rho r^2}, \quad (5)$$

$$\frac{\partial e}{\partial t} = \frac{p}{\rho^2} \frac{\partial \rho}{\partial t} - \varepsilon_{\nu}, \quad (6)$$

$$\frac{\partial (1/\mu_e)}{\partial t} = \sum_{A,Z} w_{AZ}/\mu_{AZ}, \quad (7)$$

where $m = qM$, e is the internal energy (including the binding energy of the nuclei) per unit mass, ε_{ν} is the rate of energy loss (neutrino radiation) per unit mass, $1/\mu_e$ is the number of electrons per nucleon, $1/\mu_{AZ}$ is the number of nuclei with mass number A and charge Z per nucleon, and

$$\begin{aligned} w_{AZ} = & w_{AZ}(T, \rho, \mu_e) = w_{AZ}^{-d}(T, \rho, \mu_e) + w_{AZ}^{+c}(T, \rho, \mu_e) \\ & - w_{AZ}^{-c}(T, \rho, \mu_e) - w_{AZ}^{+d}(T, \rho, \mu_e). \end{aligned} \quad (8)$$

Here w_{AZ}^{-d} , w_{AZ}^{-c} denote the rates of electron decay and capture by nuclei; w_{AZ}^{+d} , w_{AZ}^{+c} , the corresponding rates for positrons¹⁾ (free protons and neutrons are included in the number of nuclei).

In hydrostatic-equilibrium evolution the right-hand member of Eq. (4) will vanish. According to Eqs. (2) and (3), Eq. (5) will be satisfied identically for our adopted density profile (1), because the relation

$$\langle \rho \rangle = \frac{M}{4\pi R^3 \rho_c} = \frac{\mu_1}{[\psi(1)]^3} \quad (9)$$

holds for any polytropic index.¹ Since the adiabatic index in the star is not exactly equal to $4/3$, Eq. (4) with the density profile (1) cannot be satisfied at every point of the star [the pressure $p = p(T, \rho, \mu_e)$ is evaluated from the exact thermodynamic equations]. Multiplying this equation by $\partial r/\partial t$, integrating it over the entire mass of the star, and applying the method of integration by parts, we obtain

$$\frac{d}{dt} \int_0^M \frac{1}{2} \left(\frac{\partial r}{\partial t} \right)^2 dm - \frac{d}{dt} \int_0^M \frac{Gm dm}{r} = \int_0^M p \frac{\partial}{\partial t} \left(\frac{1}{\rho} \right) dm. \quad (10)$$

Equation (10) is nothing but the law for the variation of mechanical energy for the whole star.²⁾ For our adopted density profile we may require that Eq. (10) be satisfied exactly. Then the two partial differential equations (4), (5) will reduce to a single ordinary differential equation for the function $R(t)$:

$$R(t) \int_0^1 \left[\frac{\psi(q)}{\psi(1)} \right]^2 dq = \frac{3}{R(t)} \int_0^1 \frac{p}{\rho} dq - \frac{GM}{R^2(t)} \int_0^1 \left[\frac{\psi(1)}{\psi(q)} \right] q dq. \quad (11)$$

It can readily be obtained from Eq. (10) by noting that, according to Eq. (9), $\dot{\rho}_c(t)/\rho_c(t) = 3 \dot{R}(t)/R(t)$.

Before examining Eqs. (6) and (7), we have one fur-

ther remark. In principle the polytropic approximation can be employed in different ways. Fowler and Hoyle¹⁵ have used the polytropic approximation also to calculate the late evolutionary stages of massive stars. But instead of the integral relation (11) they apply the pressure equation from the exact equation of state to the polytropic pressure at the central point of the star, for which the equations of temperature variation are then written. This treatment is evidently more accurate in terms of the polytropic approximation, as the law for the variation of the total energy of the star is employed explicitly, and the temperature and chemical composition are calculated at each point of the star.

3. EQUATION OF STATE AND KINETICS OF THE β PROCESSES

Nearly the entire iron core that is formed²⁻⁴ will have a temperature $T > 2 \cdot 10^{90}$ K. If the temperature is raised to $T \gtrsim 3 \cdot 10^{90}$ K, the rate of all the nuclear processes will increase sharply, and the chemical composition of the plasma will be determined by statistical equilibrium over the nuclei¹⁶ for specified T , ρ , and μ_e :

$$N_{AZ} = \omega_{AZ} 2^{-A} A^{3/2} \left(\frac{2\pi\hbar^2}{m_p kT} \right)^{3(A-1)/2} N_n^{A-Z} N_p^Z \exp(E_{AZ}/kT), \quad (12)$$

$$\sum_{A,Z} ZN_{AZ} + N_p = \rho / \mu_e m_p, \quad (13)$$

$$\sum_{A,Z} AN_{AZ} + N_n + N_p = \rho / m_p. \quad (14)$$

Here N_{AZ} denotes the number of nuclei with the mass number A and charge Z per unit volume, ω_{AZ} is their statistical weight, N_p and N_n denote the number of free protons and neutrons per unit volume, and $E_{AZ} = (A - Z)m_{nc}^2 + Zm_{pc}^2 - m_{AZ}c^2$ is the binding energy of a nucleus. Equations (13) and (14) represent the condition of electrical neutrality and the identification of the density of matter with the number of baryons.

For each set of values of T , ρ , and μ_e , we have solved the system (12)–(14) for 10 kinds of nuclei: He^4 and nine nuclei with maximal binding energy and values of Z/A close to $1/\mu_e$. In the case of large μ_e values, where the limit of stability of nuclei against neutron decay is approached,¹⁷ the unknown binding energy has been computed from the Myers–Swiatecki equation.¹⁸ Although the system (12)–(14) has been solved for 10 kinds of nuclei, our choice of nine of them in effect enables us to monitor the density of about 30 kinds of nuclei. Calculations by the method described above yield results similar to those obtained by Clifford and Tayler.¹⁹ The chemical composition is determined by Eqs. (12)–(14) if the condition $T \geq 3 \cdot 10^{90}$ K is satisfied. For $T < 3 \cdot 10^{90}$ K the matter is assumed to consist of two kinds of nuclei for which the binding energy is maximal and at the same time Z/A is close to $1/\mu_e$ ($Z_1/A_1 < 1/\mu_e < Z_2/A_2$). This assumption is in part justified³ by the circumstance that it does not entail so marked a discontinuity in the chemical composition at $T = 3 \cdot 10^{90}$ K.

The contribution to the internal energy $e(T, \rho, \mu_e) = e_n + e_e + aT^4/\rho$ and pressure $p(T, \rho, \mu_e) = p_n + p_e + aT^4/3$ from nondegenerate nuclei and free nucleons, electron-positron gas, and radiation has been taken into account according to the standard expressions¹⁶ (the energy of the

nuclear component is measured from the rest energy of the neutrons):

$$e_n(T, \rho, \mu_e) = \frac{1}{\rho} \left[\frac{3}{2} \left(\sum_{A,Z} N_{AZ} + N_p + N_n \right) kT - \sum_{A,Z} E_{AZ} N_{AZ} - 2.53 m_e c^2 \frac{\rho}{\mu_e m_p} \right], \quad (15)$$

$$e_e(T, \rho, \mu_e) = 8\pi \frac{m_e c^2}{\rho} \left(\frac{m_e c}{2\pi\hbar} \right)^3 \times \int_1^\infty e^{\nu} \sqrt{e^2 - 1} \left\{ \frac{1}{1 + \exp[(\varepsilon - \varphi_e)/\lambda]} + \frac{1}{1 + \exp[(\varepsilon + \varphi_e)/\lambda]} \right\} d\varepsilon, \quad (16)$$

$$p_n(T, \rho, \mu_e) = \left(\sum_{A,Z} N_{AZ} + N_p + N_n \right) kT, \quad (17)$$

$$p_e(T, \rho, \mu_e) = \frac{8\pi}{3} \left(\frac{m_e c}{2\pi\hbar} \right)^3 m_e c^2 \times \int_1^\infty (e^2 - 1)^{3/2} \left\{ \frac{1}{1 + \exp[(\varepsilon - \varphi_e)/\lambda]} + \frac{1}{1 + \exp[(\varepsilon + \varphi_e)/\lambda]} \right\} d\varepsilon. \quad (18)$$

Here $\lambda = kT/m_e c^2$; $m_e c^2 \varphi_e$ represents the chemical potential of the electrons with allowance for rest mass, as given by the equation

$$\rho = \mu_e m_p 8\pi \left(\frac{m_e c}{2\pi\hbar} \right)^3$$

$$\times \int_1^\infty e^{\nu} \sqrt{e^2 - 1} \left\{ \frac{1}{1 + \exp[(\varepsilon - \varphi_e)/\lambda]} - \frac{1}{1 + \exp[(\varepsilon + \varphi_e)/\lambda]} \right\} d\varepsilon. \quad (19)$$

In the numerical computations the integrals (16), (18), and (19) have been evaluated by the five-point Laguerre quadrature formula.

The energy equation (6) contains the rate ε_ν of energy loss by neutrino radiation. Since the stellar evolution under discussion here is very rapid ($\Delta t \approx 10^4$ – 10^5 sec), cooling by electron and photon heat conduction may be neglected. The cooling rate $\varepsilon_\nu = \varepsilon_{\nu\mu} + \varepsilon_{\nu\beta}$ comprises the radiation $\varepsilon_{\nu\mu}$ of plasma neutrinos and photon neutrinos plus the radiation of neutrinos through annihilation of electron-positron pairs produced by the universal Fermi interaction, together with the URCA losses $\varepsilon_{\nu\beta}$ to nuclei and free nucleons. The first three processes have been investigated in detail by Beaudet et al.²⁰ We have adopted an expression approximating these authors' calculations in the range of parameters of interest to us:

$$\varepsilon_{\nu\mu}(T, \rho, \mu_e) = \left[0.8\rho \left(\frac{T}{10^9 \text{K}} \right)^3 / \mu_e^2 + 10^{14} \left(\frac{T}{10^9 \text{K}} \right)^{10} / \rho \right] \text{erg} \cdot \text{g}^{-1} \cdot \text{sec}^{-1}. \quad (20)$$

Expressions for the cooling rate $\varepsilon_{\nu\beta}$ by the URCA process will be given below. It is justifiable to use the rather crude Eq. (20) because calculations show that the URCA process makes the primary contribution to the energy-loss rate during the terminal evolutionary phase.²¹⁻²³ In view of the local character of the energy losses, Eq. (6) transforms into a set of ordinary differential equations for each point of the star.

Equation (7) represents the kinetic equation for the β processes. The number density $N_{AZ} = \rho / m_p \mu_{AZ}$ of each kind of nucleus is here determined from the system (12)–

(14). Every β transition is either of two types: 1) the initial nucleus is even-even and the final nucleus is odd-odd; 2) the initial and final nuclei are both even-odd. (As the odd-odd nuclei have a low binding energy, they have a negligible density in statistical equilibrium, so that their contribution as initial nuclei in β processes may be neglected.) In both types of β transformation we have taken into account for each nucleus the contribution only from the permitted transition having the lowest possible threshold [this practice applies to each type of capture (electron or positron) and decay (when possible) separately]. In the case of type 1 the transition takes place from the ground state of the even-even nucleus to the lowest of the large number of closely spaced levels of the odd-odd nucleus that satisfies the selection rules. For the even-odd nuclei participating in type 2 transitions, there generally are numerous comparatively low-lying levels with a high population at $T \gtrsim 3 \cdot 10^9 \text{K}$ ($kT \gtrsim 0.25 \text{ MeV}$); from one of them a permitted transition will be possible to a similar level in the adjacent isobar. Since the values of the quantity ft are usually very uncertain, it is fully justified to take the contribution from just one level. For permitted transitions where experimental values of ft are not available we have adopted $\log ft = 5$.

The rates of the β processes and the energy loss by neutrino radiation have been evaluated from the equations^{24,22}

$$w_{AZ}^{\pm c} = \frac{\ln 2}{ft} \int_{\max(\Delta^{\pm c}, 1)}^{\infty} \frac{\varepsilon \sqrt{\varepsilon^2 - 1} (\varepsilon - \Delta^{\pm c})^2}{1 + \exp[(\varepsilon \pm \varphi_e)/\lambda]} d\varepsilon, \quad (21)$$

$$w_{AZ}^{\pm d} = \frac{\ln 2}{ft} \int_1^{\Delta^{\pm d}} \frac{\varepsilon \sqrt{\varepsilon^2 - 1} (\Delta^{\pm d} - \varepsilon)^2}{1 + \exp[-(\varepsilon \pm \varphi_e)/\lambda]} d\varepsilon, \quad (22)$$

$$\varepsilon_{\nu\beta AZ}^{\pm c} = \frac{m_e c^2}{m_p \mu_{AZ}} \frac{\ln 2}{ft} \int_{\max(\Delta^{\pm c}, 1)}^{\infty} \frac{\varepsilon \sqrt{\varepsilon^2 - 1} (\varepsilon - \Delta^{\pm c})^3}{1 + \exp[(\varepsilon \pm \varphi_e)/\lambda]} d\varepsilon, \quad (23)$$

$$\varepsilon_{\nu\beta AZ}^{\pm d} = \frac{m_e c^2}{m_p \mu_{AZ}} \frac{\ln 2}{ft} \int_1^{\Delta^{\pm d}} \frac{\varepsilon \sqrt{\varepsilon^2 - 1} (\Delta^{\pm d} - \varepsilon)^3}{1 + \exp[-(\varepsilon \pm \varphi_e)/\lambda]} d\varepsilon, \quad (24)$$

where $\Delta^{\pm c} = (m_{AZ \pm 1} - m_{AZ})/m_e$ and $\Delta^{\pm d} = (m_{AZ} - 1)m_e$. Here m_{AZ} denotes the rest mass of the nucleus, including the excitation energy of the level participating in the transition (free protons and neutrons are counted as nuclei). The Coulomb correction factor $F^{\pm}(Z, A)$ has been neglected, because the uncertainty in ft is far greater than the error introduced by the omission of $F^{\pm}(Z, A)$. It is understood in Eqs. (22) and (24) that the quantity $\Delta^{\pm d} > 1$, for otherwise $w_{AZ}^{\pm d}$ and $\varepsilon_{\nu\beta AZ}^{\pm d}$ would vanish identically. Equations (21) and (23) combine the two types of expressions given in the papers cited above for stable and radioactive nuclei individually.⁴⁾ The total rate of URCA neutrino losses will be, then,

$$\varepsilon_{\nu\beta} = \sum_{A,Z} (\varepsilon_{\nu\beta AZ}^{+c} + \varepsilon_{\nu\beta AZ}^{+d} + \varepsilon_{\nu\beta AZ}^{-c} + \varepsilon_{\nu\beta AZ}^{-d}).$$

The integrals (21)–(24) have again been evaluated by the five-point Laguerre quadrature formula.

4. RESULTS OF NUMERICAL CALCULATIONS

We have performed numerical calculations for models with masses of 1.7, 1.4, and 1.21 M_{\odot} . The initial values for the temperature and density at the center of the

first two model stars have respectively been adopted from the two calculations by Ikeuchi et al.^{3,4} of the terminal evolutionary phases. For the initial 1.21 M_{\odot} model we have taken a cool iron white dwarf with a central density exceeding the threshold value $\rho_{\text{thr}} = 9.06$ for e^- capture by Fe^{56} nuclei. Explicitly, these initial values are $(\log T_c, \log \rho_c) = (9.544, 8.35)$, $(9.6, 8.8)$, and $(8.0, 9.5)$. The initial distribution of temperature over the mass of the star has been specified in the form $T/T_c = (\rho/\rho_c)^{\alpha}$, where the exponent α has been so selected as to yield the required value of the mass from the relation (9) and Eq. (11) in the hydrostatic case. The values of α computed in this manner lie within the range $0.1 \leq \alpha \leq 0.2$; thus the temperature varies weakly within the star, as is perfectly reasonable for these models.

Our calculations demonstrate that the stars will contract with ever increasing speed because of the drop in pressure as the number of electrons per nucleon decreases. This behavior will result from e^- captures, which play a predominant role among the β processes. Figure 1 illustrates the evolutionary tracks of the centers of the stars in the $(\log T_c, \log \rho_c)$ plane. The dashed curves in this diagram represent contours of equal values of the adiabatic index $\gamma_1 = \partial \ln p / \partial \ln \rho$ for $s = \text{const}$ and $\mu_e = \text{const}$, as introduced in a previous paper.⁹ Its value here has been computed for $\mu_e = 56/26$, which corresponds to our initial conditions.

It is apparent from Fig. 1 that the central regions of the star enter the instability well, where the index $\gamma_1 < 4/3$. The track of the 1.7 M_{\odot} star penetrates most deeply into the well. In this case the contraction of the star takes on the character of a hydrodynamic collapse because of photodisintegration processes of heavy nuclei, as follows from the discussion above. But it is a rather complicated matter to establish the point of onset of the hydrodynamic collapse phase from Fig. 1, for in the first place the index γ_1 should be less than $4/3$ within a certain zone of the star, not just at its center; and secondly, a constant value of μ_e provides too rough a description of the thermodynamic state of the material during the collapse of the star. Figure 2 shows how μ_e depends on ρ_c in these models. The increase in the electron molecular weight μ_e is fairly substantial, the more so as the mass of the star diminishes, because of the increasing role of e^- captures.

The transition to the hydrodynamic collapse phase and the evolutionary time scales are illustrated in Fig. 3. Here the rate of evolution $R^{-1} dR/dt$ is plotted as a function of the central density ρ_c . When the characteristic evolution time $(R^{-1} dR/dt)^{-1}$ becomes comparable to the hydrodynamic time $t_h = (G\rho_c)^{-1/2}$ in the course of the calculations, we introduce the hydrodynamic part of the program [taking into account the term in the left-hand member of Eq. (11)] and proceed to calculate a portion of the collapse phase.⁵⁾ The bend in the curves for $M = 1.7 M_{\odot}$ and $M = 1.4 M_{\odot}$ marks the transition to the hydrodynamic phase. At $\rho_c = 1.8 \cdot 10^9 \text{ g/cm}^3$ and $T_c = 7.4 \cdot 10^9 \text{ K}$ (see Fig. 1) the 1.7 M_{\odot} star suffers collapse through photodissociation of heavy nuclei. For the 1.8 M_{\odot} star the corresponding parameters have larger values: $\rho_c = 5 \cdot 10^9 \text{ g/cm}^3$ and $T_c = 9 \cdot 10^9 \text{ K}$ (the calculation was terminated at this epoch for the 1.4 M_{\odot} model).

The situation is completely different for the collapse

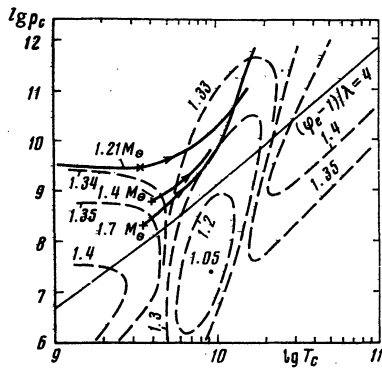


Fig. 1. Solid curves, density and temperature variation at the center of three model stars during the contraction process. Dashed curves, contours of equal values of the adiabatic index $\gamma_1 = \partial \ln p / \partial \ln \rho$ for $s = \text{const}$ and $\mu_e = 56/26$. Along the thin line the degeneracy parameter of the electron gas $(\phi_e - 1)/\lambda = 4$.

of the star of lowest mass, $1.21 M_\odot$. Here the central regions of the star do enter the instability well (Fig. 1), but this penetration is no longer accompanied by a loss of mechanical stability. The evolution of the star proceeds at the characteristic rate $\mu_e^{-1} d\mu_e/dt$ of the β processes. When the Fermi energy E_F of the relativistically degenerate electron gas [the degeneracy is continually strong; Fig. 1 displays the line $(\phi_e - 1)/\lambda = 4$] substantially exceeds the threshold capture energy, then the β -process rate

$$\frac{1}{\mu_e} \frac{d\mu_e}{dt} \propto E_F^3 \propto (\rho/\mu_e)^{3/2}$$

In Fig. 3 this relationship is indicated by the dot-dash line. We see that in the $1.21 M_\odot$ case the rate of evolution increases with density far more rapidly than the hydrodynamic rate ($t_h^{-1} \propto \rho^{1/2}$). Thus the evolution with the characteristic time scales of the β processes undergoes a smooth transition to the collapse phase, unlike the case for the more massive stars (1.7 and $1.4 M_\odot$), where mechanical stability is lost at a sharply defined epoch.

We have found from the calculations that even for the comparatively low initial value of the central density ($\rho_c < \rho_{\text{thr}}$) in the $1.7 M_\odot$ model, the influence of β processes on the evolution cannot be neglected. Figure 4 shows the proportionate contribution $\epsilon_{\nu\beta}/\epsilon_\nu$ of all URCA losses and the contribution $\epsilon_{\nu\beta n}/\epsilon_\nu$ of URCA losses to free nucleons at the center of the star. We observe that the URCA processes have a large contribution at the very outset and that it increases rapidly with ρ_c and T_c . For $M = 1.7 M_\odot$ the cooling rate is dominated by URCA losses through capture of electrons by protons when $T_c \gtrsim 6 \cdot 10^9 \text{ K}$ ($\rho_c \gtrsim 10^9$

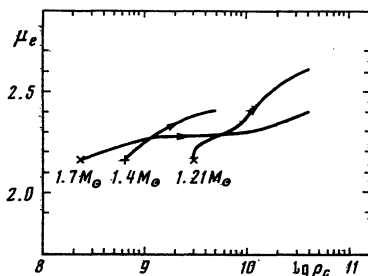


Fig. 2. Variation in the electron molecular weight μ_e at the center of the three model stars ($1/\mu_e$ is the number of electrons per nucleon).

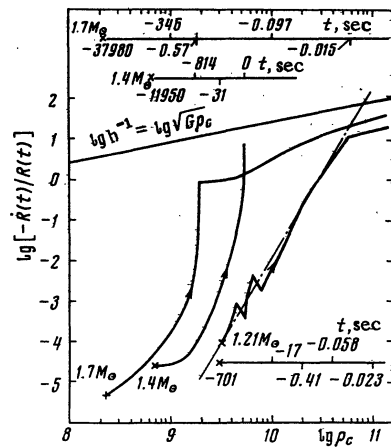


Fig. 3. Variation of the evolution rate $\dot{R}(t)/R(t)$ during collapse. The characteristic free-fall rate $t_h^{-1} = (G\rho_c)^{1/2}$ is indicated for comparison. Time scales are shown for each of the three models.

g/cm^3); in fact, the contribution of all other mechanisms is insignificant. For $M = 1.21 M_\odot$ the predominant role of e^- capture by protons sets in when $\rho_c \gtrsim 5 \cdot 10^9 \text{ g/cm}^3$.

Because of the nonequilibrium character of the e^- captures, the increase in the energy-loss rate is not accompanied by a more rapid decline in entropy. Figure 5 displays the change in entropy (in units of k per nucleon) as ρ_c rises. Curves for the quantity $m_p \int (\epsilon_\nu/kT) dt$ are

included in the diagram. If the β processes operated in equilibrium, the sum of these quantities would evidently remain constant. When we say that the β processes are nonequilibrium mechanisms, we mean that not only thermodynamic equilibrium is violated (neutrinos can in fact escape freely from the star, and the entropy will no longer be related to the energy losses by the ratio mentioned above^{24,25}), but also the kinetic equilibrium of the β processes^{24,25} Symbolically, such an equilibrium would imply that the relation $w^{-c} + w^{+d} = w^{+c} + w^{-d}$ is satisfied, but our calculations demonstrate that kinetic equilibrium is never established, not even for the $1.7 M_\odot$ model and certainly not for the lower-mass models. Actually we always have $w^{-c} + w^{+d} \gg w^{+c} + w^{-d}$, with electron captures predominating.

This result can be explained quite simply. In a non-steady process, whatever the values of ρ and T the quantity μ_c should be smaller than would be the case in kinetic equilibrium. Hence the chemical potential of the electrons

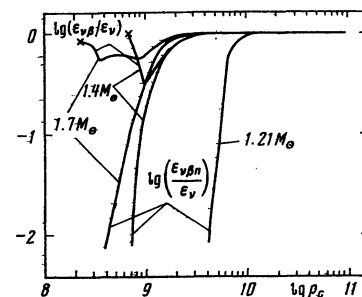


Fig. 4. Relative contribution of different energy-loss mechanisms. ϵ_ν , total losses by neutrino radiation; $\epsilon_{\nu\beta}$, URCA losses; $\epsilon_{\nu\beta n}$, URCA losses to free nucleons.

TABLE 1

Element	p	n	He ⁴	Cr ⁵⁴	Ti ⁵⁰	Fe ⁶⁰	Fe ⁵⁸	Ni ⁶⁶	Cr ⁵⁶	Ni ⁶⁴	Cr ⁵³	Fe ⁵⁷
$1/\mu_{AZ} \cdot 10^4$	0.14	13	22	48	35	26	22	14	13	9.6	5.3	3.1

(and accordingly the degree of degeneracy) will conversely be larger than its equilibrium value. As a consequence the positron density will diminish very substantially for even a slight difference in the chemical potential (under conditions of strong degeneracy; see Fig. 1), so that the principal compensatory process w^+c will virtually disappear. It is this situation that has been demonstrated by our calculations.

A growth of entropy (if other conditions are the same) will facilitate the attainment of higher temperatures in the central zone of the star for a given density, and thereby the instability well $\gamma_1 < 4/3$ (Fig. 1) will be penetrated more deeply. Since the entropy continually increases (Fig. 5), especially in the $1.21 M_\odot$ case (for which nonequilibrium β processes have the strongest influence), the star will collapse only because of the drop in pressure due to e^- captures (see the graph of Fig. 2 for the variation in μ_e at the center of the star).

The chemical composition of the central regions of the star will be determined by statistical equilibrium among the nuclei for given T , ρ , and μ_e . Over the course of the evolution, as well as during the hydrodynamic phase, heavy-element nuclei will comprise the predominant portion of the nucleons. The abundance of free protons will be extremely small and can never exceed 10^{-3} per nucleon. As an illustration we give in Table 1 the chemical composition at the center of the $1.7 M_\odot$ star for the epoch when stability is lost ($1/\mu_{AZ}$ denotes the number of nuclei of an element per nucleon).

An important shortcoming of the approximations adopted in this paper is the circumstance that, for a specified density profile, loss of stability and collapse of a certain portion of the star cannot take place in our models. Thus we cannot investigate the possible formation of neutron stars whose mass $M \approx 0.3-0.7 M_\odot$ is considerably lower than the Chandrasekhar limit M_{Ch} . If the critical adiabatic index $4/3$ is reached in a nucleus whose mass M exceeds a critical value⁶ $M_{Cr} > M_{Ch}$, the nucleus

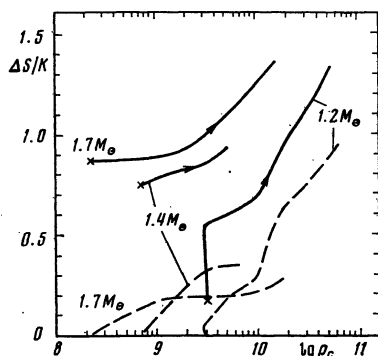


Fig. 5. Change in entropy at the center of the star. Solid curves, entropy increment ΔS per nucleon in units of the Boltzmann constant k ; dashed curves, energy-loss integral per nucleon, $m_p \int_0^1 (\epsilon_\nu/kT) dt$.

will unequivocally collapse whether an outer envelope is present or not, while this will not be the case if $M < M_{Ch}$. When $M < M_{Ch}$ the envelope lying above M plays a fundamental role. The smaller the ratio M/M_{Ch} , the stronger should be the pressure of the envelope on M and the greater the difference $4/3 - \langle \gamma \rangle$ in order for the mass M to be able to contract to the neutron-star state. Very likely before the conditions necessary for the loss of stability of the mass M are achieved, weaker conditions can be satisfied that will suffice for the collapse of some mass M_1 such that $M < M_1 \approx M_{Ch}$. Among the models we have investigated, the most favorable conditions for collapse of a small mass occur in the $1.21 M_\odot$ star, where the central zone enters the $\gamma_1 < 4/3$ well, and moreover where hydrostatic-equilibrium evolution proceeds to the high-density (and hence high-pressure) limit $\rho_c \approx 10^{11} \text{ g/cm}^3$.

5. PRINCIPAL CONCLUSIONS

If during the terminal phase in the nuclear evolution of a star an iron core is formed with a mass in the range $1.21 \leq M \leq 1.7 M_\odot$, then the core will subsequently contract with increasing speed and will ultimately collapse, producing a neutron star or a black hole. For the higher masses ($M = 1.7$ and $1.4 M_\odot$), the transition to the collapse phase bears the sharply defined character of a loss of mechanical stability throughout the star because of photodissociation of the heavy elements. For the lowest mass considered ($M = 1.21 M_\odot$), there is a smooth transition; the evolution on the characteristic time scale of the β processes gradually accelerates, practically up to the free-fall state. In all the models we have examined the possibility is in principle present that at the center of the collapsing star a neutron star may form whose mass does not exceed its maximum limit of $\approx 1.7-2.0 M_\odot$.

In the terminal evolutionary phase β processes play the most important role. Neutrinos radiated through e^- capture make a major contribution to the cooling rate, and when $T \gtrsim 6 \cdot 10^9 \text{ K}$ electron capture by free protons will predominate. Because of the nonequilibrium character of the e^- capture, the entropy of the central regions of the star will increase during the contraction process. The collapse of the star results from the pressure drop due to the decrease in the number of particles when e^- captures take place.

The authors are indebted to G. S. Bisnovatyi-Kogan and V. M. Chechëtkin for engaging in many discussions and offering valuable comments.

¹) When positrons are taken into account, the value of $1/\mu_e$ will evidently be equal to the difference between the number of electrons and positrons per nucleon.

²) By means of the first law of thermodynamics [Eq. (6)], $p \partial(1/\rho)/\partial t = -\partial \epsilon / \partial t - \epsilon_\nu$, Eq. (10) can clearly be transformed into a law for conservation of the total energy of the star.

³) One should, in fact, calculate the kinetics of the nuclei due to β processes and nuclear reactions. But this complicated procedure would hardly be war-

ranted in view of the slight effect of such a refinement in the peripheral regions of the star where computations show that T is indeed less than $3 \cdot 10^9$ K, upon the evolution of the star as a whole.

⁴The equation $\Delta^{+c} = -\Delta^{+d}$ holds. In the case of a radioactive nucleus (e^- decay), $\Delta^{-d} > 1$; hence $\Delta^{+c} < -1$, and e^+ capture with no threshold will be possible. As before, however, such capture can also take place if $1 > \Delta^{-d} > -1$ ($-1 < \Delta^{+c} < 1$), when only K capture is possible under laboratory conditions. If $\Delta^{-d} < -1$ we will now have $\Delta^{+c} > 1$, so that e^+ capture will proceed from a threshold [the lower limit of the integrals (21) and (23) will be Δ^{+c}], and in a given pair of nuclei, (A, Z) and $(A, Z+1)$, K capture and e^+ decay will be possible [$(A, Z+1) \rightarrow (A, Z)$]. Similar considerations may be advanced for the other pair of nuclei, (A, Z) and $(A, Z-1)$.

⁵We would again emphasize that the density profile we have used becomes most inaccurate in the hydrodynamic collapse phase as the kinetic energy of the material increases.

⁶ $M_{Cr} = M_{Ch}$ when the entropy $S(q) \equiv 0$ throughout the star; if $S(q) > 0$ we will always have $M_{Cr} > M_{Ch}$.

¹Ya. B. Zel'dovich and I. D. Novikov, *Relativistic Astrophysics*, Vol. 1, Stars and Relativity, Univ. Chicago Press (1971).

²G. Rakavy, G. Shaviv, and Z. Zinamon, *Astrophys. J.*, **150**, 131 (1967).

³S. Ikeuchi, K. Nakazawa, T. Murai, R. Hōshi, and C. Hayashi, *Progr. Theor. Phys. (Japan)*, **46**, 1713 (1971).

⁴S. Ikeuchi, K. Nakazawa, T. Murai, R. Hōshi, and C. Hayashi, *Progr. Theor. Phys.*, **48**, 1870 (1972).

⁵V. I. Varshavskii and A. V. Tutkov, *Nauch. Inform. Astron. Soveta Akad. Nauk SSSR*, No. 23, 47 (1972); No. 26, 35 (1973).

⁶B. Paczynski, Preprint No. 1, Polish Acad. Sci., Warsaw (1971).

⁷V. S. Imshennik and D. K. Nadēzhin, in: *Late Stages of Stellar Evolution*

(IAU Sympos. No. 66), Reidel (1974), p. 130; *Nauch. Inform. Astron. Soveta Akad. Nauk SSSR*, No. 29, 27 (1974).

⁸Z. Barkat, J. C. Wheeler, J.-R. Buchler, and G. Rakavy, *Astrophys. Space Sci.*, **29**, 267 (1974).

⁹V. S. Imshennik and V. M. Chechētkin, *Astron. Zh.*, **47**, 929 (1970) [*Sov. Astron.*, **14**, 747 (1971)].

¹⁰G. S. Bisnovatyι-Kogan and Z. F. Seidov, *Astron. Zh.*, **47**, 139 (1970) [*Sov. Astron.*, **14**, 113 (1970)].

¹¹D. Sugimoto, *Astrophys. J.*, **161**, 1069 (1970).

¹²T. Hamada and E. E. Salpeter, *Astrophys. J.*, **134**, 683 (1961).

¹³K. Nakazawa, *Progr. Theor. Phys.*, **49**, 1932 (1973).

¹⁴G. S. Bisnovatyι-Kogan, *Astron. Zh.*, **45**, 74 (1968) [*Sov. Astron.*, **12**, 58 (1968)].

¹⁵W. A. Fowler and F. Hoyle, *Astrophys. J. Suppl.*, **9** (No. 91), 255 (1964).

¹⁶V. S. Imshennik and D. K. Nadēzhin, *Astron. Zh.*, **42**, 1154 (1965) [*Sov. Astron.*, **9**, 896 (1966)].

¹⁷P. É. Nemirovskii, *Zh. Eksp. Teor. Fiz.*, **36**, 889 (1959) [*Sov. Phys. - JETP*, **9**, 627 (1959)].

¹⁸W. D. Myers and W. J. Swiatecki, *Nucl. Phys.*, **81**, 1 (1966).

¹⁹F. E. Clifford and R. J. Taylor, *Mem. Roy. Astron. Soc.*, **69**, 21 (1965).

²⁰G. Beaudet, V. Petrosian, and E. E. Salpeter, *Astrophys. J.*, **150**, 979 (1967).

²¹D. K. Nadēzhin and V. M. Chechētkin, *Astron. Zh.*, **46**, 270 (1969) [*Sov. Astron.*, **13**, 213 (1969)].

²²G. Beaudet, E. E. Salpeter, and M. L. Silvestro, *Astrophys. J.*, **174**, 79 (1972).

²³L. N. Ivanova, V. S. Imshennik, and D. K. Nadēzhin, *Nauch. Inform. Astron. Soveta Akad. Nauk SSSR*, No. 13, 3 (1969).

²⁴V. S. Imshennik, D. K. Nadēzhin, and V. S. Pinaev, *Astron. Zh.*, **44**, 768 (1967) [*Sov. Astron.*, **11**, 617 (1968)].

²⁵V. M. Chechētkin, Candidate's Dissertation, Inst. Appl. Math. USSR Acad. Sci., Moscow (1970).